Applied Thermal Engineering 67 (2014) 370–377

Contents lists available at ScienceDirect

Applied Thermal Engineering

journal homepage: www.elsevier.com/locate/apthermeng

Transient modeling of high-inertial thermal bridges in buildings using the equivalent thermal wall method

F. Aguilar [a], J.P. Solano [b], P.G. Vicente [a,*]

[a] Universidad Miguel Hernández, Departamento de Ingeniería Mecánica y Energía, Avenida de la Universidad, 03202 Elche, Spain
[b] Universidad Politécnica de Cartagena, Departamento de Ingeniería Térmica y de Fluidos, Campus Muralla del Mar, 30202 Cartagena, Spain

HIGHLIGHTS

- Two highly-inertial thermal bridges are analyzed using the equivalent thermal wall method.
- We present a method for obtaining the thermal properties of the equivalent walls.
- A strategy for the decomposition of the thermal bridges into several walls is devised.
- The transient performance of the equivalent thermal walls is compared with classical models.
- A reliable analysis of the transient thermal performance through thermal bridges is demonstrated.

GRAPHICAL ABSTRACT

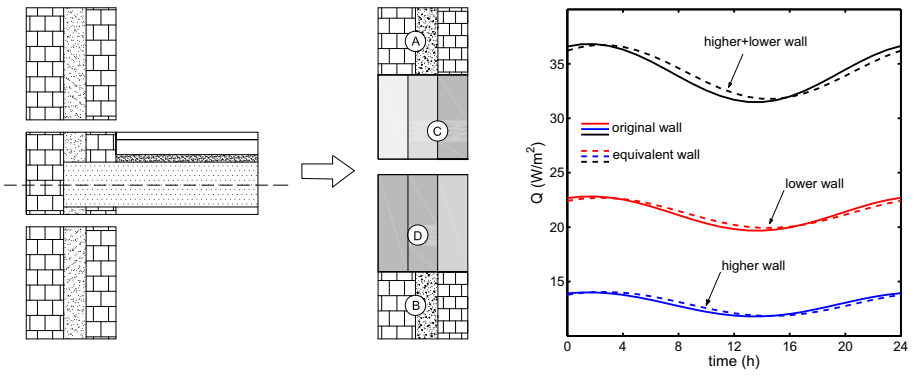

ARTICLE INFO

Article history:
Received 23 August 2013
Accepted 23 March 2014
Available online 3 April 2014

Keywords:
Thermal bridge
Equivalent thermal wall
High thermal inertia
Numerical heat conduction

ABSTRACT

The method of the equivalent thermal wall has been employed for modeling the transient response of high-inertial thermal bridges. A new strategy is presented in order to adjust the thermal properties of the equivalent three-layered wall, which takes into account the temperature distribution across the thermal bridge in a steady-state heat conduction scenario. Two different thermal bridge topologies created by the junction of a vertical wall and an intermediate or a ground floor slab are analyzed with this method, and its feasibility for the implementation in building energy simulation tools is discussed: if the thermal bridge is not considered, an underestimation of 25% in the heat flux across the bridge is predicted. If the thermal bridge is modeled but its thermal inertia is neglected, a time-delayed heat flux response is retrieved. Conversely, the simulation based on the equivalent wall method provides a response nearly identical to the actual dynamic performance of the thermal bridge.

1. Introductions

The basic requirement to limit the energy consumption, as prescribed in the European Directive 2002/91/EC on the energy performance of buildings [1], provides the principles to safeguarding comfortable indoor climatic conditions while controlling the energy demand. An appropriate thermal insulation is among the main measures to reduce the energy consumption in buildings. Regarding this issue, Al-Sanea and Zedan [2] analyzed the importance of the thermal insulation and its correct location in building envelopes. However, even a well insulated construction may be subjected to substantial energy losses, owing to the complex

* Corresponding author. Tel.: +34 966 658 561.
E-mail address: pedro.vicente@umh.es (P.G. Vicente).

http://dx.doi.org/10.1016/j.applthermaleng.2014.03.058
1359-4311/

Nomenclature

A	surface of the thermal bridge (m^2)
C	heat capacity (m^2 K W^{-1})
C_p	specific heat (J kg^{-1} K^{-1})
dV	differential volume (m^3)
E	energy stored in the thermal bridge (J)
e	layer thickness (m)
H	distance from the adiabatic plane to each side of the thermal bridge junction (m)
k	thermal conductivity (W m^{-1} K^{-1})
L_{TB}	length of influence of the thermal bridge (m)
L_W	length of the wall unaffected by the thermal bridge (m)
Q	heat (W)
q	heat flux (W m^{-2})
R	thermal resistance (m^2 K W^{-1})
S	boundary of the thermal bridge (m)
t	time (s)
T_n	temperature of the differential element (°C)
T_i	inner temperature of an enclosure (°C)
T_o	outside temperature of an enclosure (°C)
ΔT	temperature difference across the thermal bridge, $T_i - T_o$ (°C)
U	thermal transmittance (W m^{-2} K^{-1})
X	heat fraction through the thermal bridge (−)
x	horizontal coordinate (m)
y	vertical coordinate (m)

Greek symbols

α	thermal diffusivity (m^2 s^{-1})
φ	dimensionless factor of the equivalent thermal wall (−)
Ψ	linear heat transfer coefficient (W m^{-1} K^{-1})
ρ	density (kg m^{-3})

Subscripts

ext	external layer
f	façade
h	higher wall
i	inside
int	internal layer
l	lower wall
m	m-th layer
o	outside
s	slab
TB	thermal bridge

configurations, joints and assemblies known as thermal bridges, where the continuity of the insulation is broken. Owing to the lower overall thermal resistance and the associated energy losses, the appropriate analysis of thermal bridges is of primary importance to evaluate accurately the energy demand in buildings. This need not only extends to new constructions but also to old buildings. For example, the double wall construction, usually employed in the past in the south of Europe, is rather susceptible to the occurrence of thermal bridges. The analysis of the thermal bridges impact will in that sense also highlight the potential for energy renovation measures like retrofitting of insulation in older buildings.

The international standard ISO 10211 [3,4] compiles the guidelines for the calculation of thermal bridges in building construction. Additionally, there exist national standards in most of the countries of the EU, which expand on the methodology and requirements for their calculation.

A basic approach for the energy assessment of buildings involves the omission of the thermal bridges and their effects. The outcome of this method only takes into account the heat transfer across the building envelope. A second option consists of modeling the thermal bridges as a linear heat transfer resistance, which is only a function of the thermal bridge length and the temperature difference between the indoor and outside conditions. This method requires the definition of the linear parameter Ψ (W/mK), and does not take into account the thermal inertia of the thermal bridge. In spite of the available software for the calculation of Ψ (e.g., KOBRA, THERM), most of the national building standards provide with tabulated values for different configurations. A most accurate method consists of modeling the thermal bridges as a solid mass with thermal inertia. Albeit more complex, this is a more realistic option for the analysis of thermal loads and energy demand in buildings. Following the latter approach, the Intelligent Energy Europe project ASIEPI [5] supports the use of simulation codes rather than the application of default values obtained from simplified methods. However, the inherent complexity of the transient simulation of thermal bridges frequently results in the analysis of steady-state problems or the use of tabulated quantities. An alternative to the full envelope simulation is the analysis of the transient heat conduction across simplified models, which would dramatically reduce the complexity of the simulation and the computational cost of the problem. Gao et al. [6] progressed on the transient analysis of simplified models from three-dimensional thermal bridges. Likewise, Karambakkam et al. [7] proposed the method of the homogeneous layered wall to obtain simpler models from complex wall configurations. The equivalent thermal wall method, widely developed by Kossecka and Kosny [8,9], consists of a simplification method to obtain multi-layered walls from thermal bridges with complex geometry. The equivalent wall presents the same thermal performance of the original thermal bridge, both in steady-state and dynamic conditions. Instead of performing the laborious simulation of the full thermal bridge, the method of the equivalent thermal wall allows to analyze the problem of heat conduction across a three-layered wall, with known analytical solution [10].

In the present work, a novel technique to simplify highly inertial thermal bridges is developed, based on the equivalent thermal wall method. This technique relies on the calculation of the thermal properties of the three-layered equivalent wall by means of an iterative algorithm proposed by the authors. Two different thermal bridge topologies created by the junction of a vertical wall and an intermediate or a ground floor slab are subsequently studied, in light of the easy tailoring of these geometries to a wide range of 2D configurations that yield highly-inertial thermal bridging in buildings. A methodology for the decomposition of these geometries into their equivalent thermal walls is duly described. The method allows to solve efficiently the dynamic response of thermal bridges with high thermal inertia, considering their influence in the calculation of both the thermal load and the energy demand of the building. This method can be implemented in building energy simulation programs like Energy Plus [11,12] or DOE-2 [13], being the equivalent walls composed of three-layered enclosures which allow for a fast and accurate calculation.

2. Calculation method

In order to obtain the simplified model of a thermal bridge, three different steps are required: a) the solution of the steady-state heat conduction problem across the element, in order to retrieve the temperature distribution and wall heat fluxes; b) the calculation of the dimensionless factors that drive the definition of the equivalent thermal wall, following the method of Kossecka and Kosny [8,9]; c) the assessment of the thermal properties of the three-layered equivalent thermal wall.

2.1. Numerical heat conduction problem

The two-dimensional steady state heat conduction problem in the cross section of a thermal bridge is governed by the Laplace equation Eq. (1). The boundary conditions depicted in Eq. (2) account for the thermal resistances of the surfaces against heat convection and radiation with the surrounding mediums. The temperatures of the outside and indoor regions are prescribed respectively as $T_o = 1\,^{\circ}\mathrm{C}$ and $T_i = 0\,^{\circ}\mathrm{C}$ (the study would draw similar conclusions if other values were considered). At the interfaces (i–j) of the different layers of the enclosure, the boundary conditions implemented are presented in Eq. (3), assuming that two bodies in contact must have the same temperature at the area of contact (3a) and the heat flux on the two sides of an interface must be the same (3b).

$$\frac{\partial^2 T}{\partial x^2} + \frac{\partial^2 T}{\partial y^2} = 0, T \in \Omega \tag{1}$$

$$\left.\begin{aligned} -k_{\mathrm{ext}}\frac{\partial T}{\partial n} &= \frac{1}{R_{\mathrm{ext}}}\left(T_{\mathrm{ext}} - T_{w,e}\right) \\ -k_{\mathrm{int}}\frac{\partial T}{\partial n} &= \frac{1}{R_{\mathrm{int}}}\left(T_{\mathrm{int}} - T_{w,i}\right) \end{aligned}\right\} \tag{2}$$

$$\left.\begin{aligned} T_i &= T_j \\ -k_1\frac{\partial T}{\partial n} &= -k_2\frac{\partial T}{\partial n} \end{aligned}\right\} \tag{3}$$

Two different numerical techniques have been employed simultaneously for the solution of the steady-state heat conduction problem across the thermal bridges: the finite volume method [14,15], by means of an in-house code developed in Matlab [16]; and the finite element method, using the commercial software Ansys [17]. The similarity of both solutions serves as assessment of the validity of the results obtained. The guidelines of the international standards ISO 10211-1 [3] and ISO10211-2 [4] for the modeling and calculation of thermal bridges have been duly considered. The validation of the calculation method has been accomplished according to the criteria presented in the Annex A of ISO 10211-1 [3] for 2D geometries. Differences lower than 0.1 K between the numerical and the listed solutions are obtained, which certifies the high accuracy of the computational method employed.

2.2. Equivalent thermal wall

The resulting wall heat flux and temperature field in the domain allow to compute the heat capacity as $C = \int_{\Omega}\rho C_p \mathrm{d}V$ and the thermal transmittancy $U = Q_{\mathrm{TB}}/(A\cdot\Delta T)$, where Q_{TB} is the total heat that penetrates the thermal bridge, A is the inner surface and $\Delta T = 1$ K. According to Kossecka and Kosny [8,9], the dimensionless factors φ_{ii}, φ_{ee}, φ_{ie} are obtained from the next expressions, which are

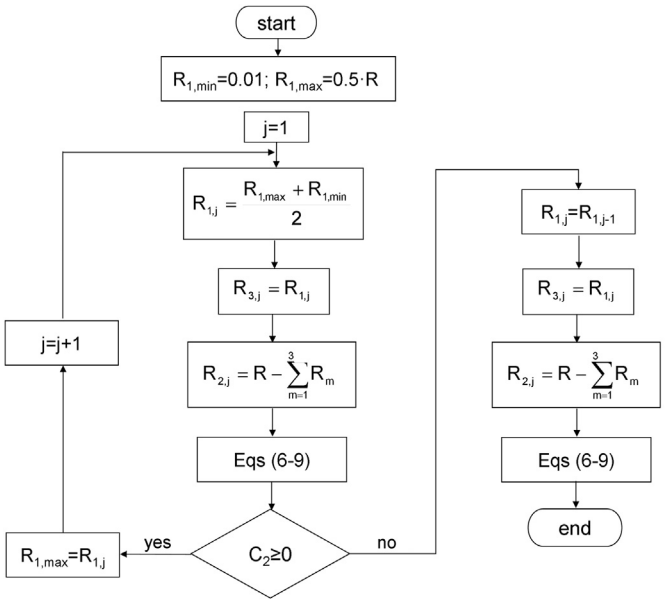

Fig. 1. Flow diagram for the calculation of the thermal properties of the equivalent thermal wall.

integrated numerically across the three-dimensional enclosure, being T_n the temperature in each node of the discretized domain:

$$\left.\begin{aligned} \varphi_{ii} &= \frac{1}{C}\int \rho C_p (1 - T_n)^2 \mathrm{d}V \\ \varphi_{ee} &= \frac{1}{C}\int \rho C_p T_n^2 \mathrm{d}V \\ \varphi_{ie} &= \frac{1}{C}\int \rho C_p (1 - T_n) \mathrm{d}V \end{aligned}\right\} \tag{4}$$

These values must satisfy the condition:

$$2\varphi_{ie} + \varphi_{ii} + \varphi_{ee} = 1 \tag{5}$$

The thermal performance of the equivalent wall can be described by the dimensionless factors φ_{ii}, φ_{ee}, φ_{ie}, the thermal transmittancy U and the heat capacity C. These quantities allow to derive, for each layer of the equivalent wall, the values C_m, R_m, ρ_m and k_m, where $m = 1, 2, 3$. It is important to note that nor the width

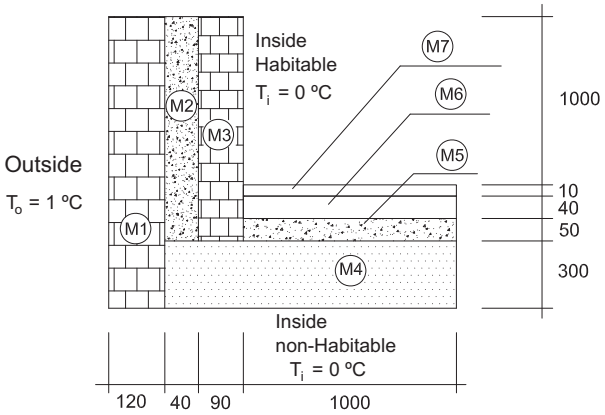

Fig. 2. Analysis of the layers of a thermal bridge created by the junction of an external façade and a lower floor slab, with non-habitable lower indoor space. Dimensions in mm.

Table 1
List of building materials and their thermal properties for cases 3.1 and 3.2 (see Figs. 2 and 7).

Label	Material	ρ (kg/m^3)	c_p (J/kg K)	k (W/m K)
M1	1/2 ft solid brick	900	1000	0.512
M2	Mineral wool	40	1000	0.041
M3	Double hollow brick	630	1000	0.212
M4	Reinforced concrete slab	1090	1000	1.22
M5	Extruded polystyrene insulation	25	1000	0.04
M6	Reinforced mortar layer	1350	800	0.7
M7	Ceramic tiles	2000	1000	1
M8	White plaster	1150	1000	0.57
M9	Acoustic insulation	40	1000	0.032

of the layers neither their specific heat play a role in the steady state heat transfer calculation. Because of this, the default values $e = 0.1$ m and $C_p = 1000$ J/kg K are considered hereafter for the three layers.

2.3. Adjustment of the thermal properties

An iterative algorithm has been developed in order to calculate the thermal variables C_m, R_m, ρ_m and k_m of the three layers that compose the equivalent thermal wall. The method consist of the search of the thermal resistance of the external layer R_1 for which the heat capacity of the intermediate level C_2 is close to zero but positive. The equations that govern the method are given by Kossecka and Kosny [8]:

$$\varphi_{ii} + \varphi_{ie} = \frac{1}{RC}\sum_{m=1}^{3} C_m\left(\frac{R_m}{2} + R_{m-o}\right) \tag{6}$$

$$\varphi_{ie} = \frac{1}{R^2C}\sum_{m=1}^{3} C_m\left(\frac{-R_m^2}{3} + \frac{R_m R}{2} + R_{i-m}R_{m-o}\right) \tag{7}$$

$$R = \sum_{m=1}^{3} R_m \tag{8}$$

$$C = \sum_{m=1}^{3} C_m \tag{9}$$

The iterative process for the calculation of the variables of interest is described in the flow diagram depicted in Fig. 1. This method can be applied directly for integrated thermal bridges, e.g., joists, cavity walls, roller shutter boxes, etc. Conversely, this is not true for thermal bridges originated by the junction of different enclosure elements. In this case, the high thermal inertia of the resulting bridge must be accounted for considering each individual enclosure. The need for an adjustment of the different thermal inertias of a bridge elements and the inertias of the equivalent wall was already claimed for by Kossecka and Kosny [8] in their introduction of the method of the equivalent thermal wall. In the present work, the methodology for the association of the thermal inertias of different enclosures is developed. This approach is presented in Section 3 using as test cases the thermal bridges originated by two classical constructive solutions: the junction of a vertical wall and an intermediate or a ground floor slab.

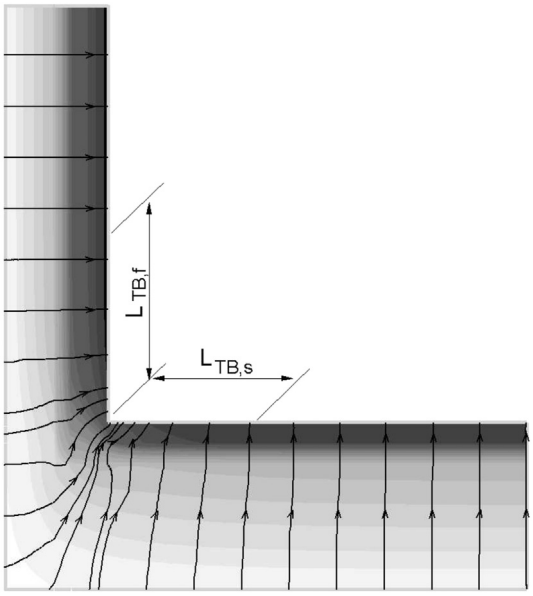

Fig. 4. Heat flow vectors across the thermal bridge.

3. Practical cases

3.1. Vertical wall and ground floor slab

Constructive details of the thermal bridge originated by the junction of a vertical wall and a ground floor slab are presented in Fig. 2. The outside surface of the vertical wall is in contact with the ambient, the upper indoor space is defined as habitable and the lower indoor space is a non-habitable highly ventilated room. The

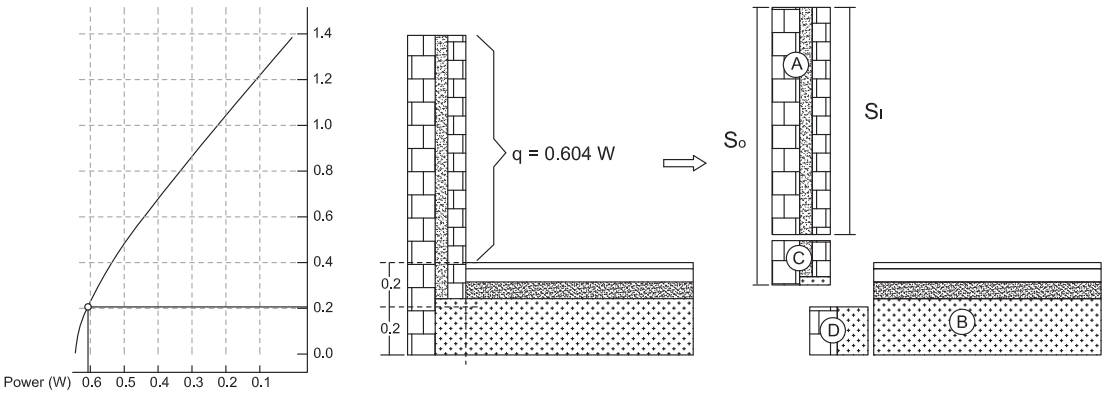

Fig. 3. Application of the method of the equivalent thermal wall on a thermal bridge created by a vertical façade and a lower floor slab.

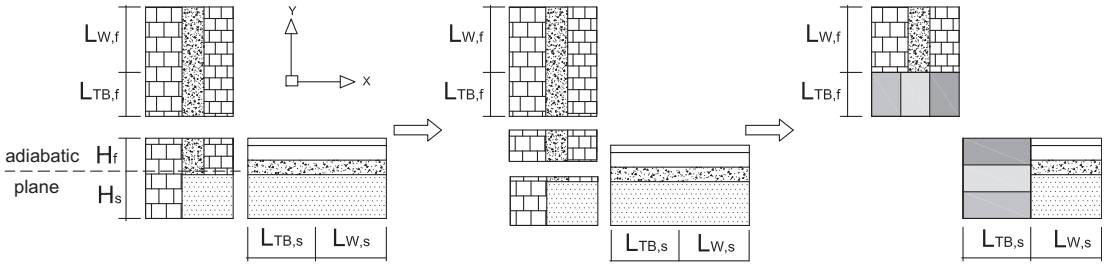

Fig. 5. Method for the adjustment of thermal inertias of the equivalent thermal wall for the junction of a façade and a lower floor slab.

adiabatic surface is defined at a distance of 1 m from the intersection of both enclosures, where the lateral heat conduction effects are negligible. The material of each component of this thermal bridge and their thermal properties are included in Table 1.

3.1.1. Adjustment of the method

As explained in Section 2, it is necessary to re-assign the thermal inertias of the thermal bridge elements. The method proposed consists of identifying the adiabatic plane, which divides the intersecting mass of the thermal bridge proportionally to its influence over the two spaces surrounding the enclosure. The location of the adiabatic plane is derived through the conservation law:

$$\int_{S_o} q_{\text{ext},x}\,dy = \int_{S_i} q_{\text{int},x}\,dy \tag{10}$$

where S_o and S_i are the outside and indoor surface boundaries of the thermal bridge, as depicted in Fig. 3. $q_{\text{ext},x}$ is the wall heat flux that enters the bridge from the external layer of the vertical wall. $q_{\text{int},x}$ is the wall heat flux that penetrates through the internal layer of the vertical wall. Both heat flux distributions are obtained from the numerical solution of the 2D steady-state heat conduction problem in the thermal bridge (see Fig. 4). The definition of the adiabatic plane allows the following description of the dimensional magnitudes of the thermal bridge, referenced to indoor levels (see Fig. 5):

- $L_{\text{TB},f}$: length of influence of the façade thermal bridge. It extends over the region where the steady-state heat flux streamlines are affected by two-dimensional effects.
- $L_{W,f}$: length of the façade wall, $L_f - L_{\text{TB},f}$
- $L_{\text{TB},s}$: length of the slab thermal bridge. It extends over the region where the steady-state heat flux streamlines are affected by two-dimensional effects.
- $L_{W,s}$: length of the slab wall, $L_s - L_{\text{TB},s}$
- H_s: Vertical distance from the base of the thermal bridge to the adiabatic plane. This dimension assesses the portion of solid in the corner of the geometry that contributes to increase the heat transfer across the slab.
- H_f: Vertical distance from the adiabatic plane to the façade wall. This dimension assesses the portion of solid in the corner of the geometry that contributes to increase the heat transfer across the façade.

The assessment of these dimensions using the steady-state temperature distribution of the thermal bridge is summarized in Table 2.

3.1.2. Results

Once the thermal bridge has been delimited by the adiabatic plane and the borders of the two-dimensional effects region, the topology of the enclosure is separated into four regions as shown in Fig. 5. Regions A and B are respectively the vertical and horizontal sectors of the thermal bridge that can be modeled as 1D multi-layered substrates. Likewise, regions C and D are the equivalent thermal walls deducted from the vertical wall and the slab floor. The suitability of the algorithm sketched in the flow diagram of Fig. 1 for the computation of the equivalent wall thermal properties is analyzed next, focusing on its appropriateness for dealing with high thermal-inertial enclosures. Tables 3 and 4 summarize the properties of the equivalent thermal wall C (vertical wall). The quantities obtained for the equivalent thermal wall D (slab floor) are reported in Tables 5 and 6.

In order to validate the simulation method, the dynamic response of the thermal bridge (Fig. 3) and its equivalent thermal wall model (Fig. 5) is analyzed. The transient heat conduction problem is modelled with the two-dimensional Fourier equation:

$$\frac{\partial^2 T}{\partial x^2} + \frac{\partial^2 T}{\partial y^2} = \frac{1}{\alpha}\frac{\partial T}{\partial t} \tag{11}$$

The same boundary conditions defined in Eqs. (2) and (3) apply here. In this situation, the outside temperature fluctuates with the law $T_{\text{ext}}(t) = F\sin(\omega t)$, where the amplitude is $F = 5$ °C is and the period is 24 h. The indoor temperature is maintained constant during the simulation, $T_{\text{int}} = 20$ °C. In order to get results

Table 2
Characteristic lengths of the thermal bridge created by lower-floor slab and façade.

	L_W (m)	L_{TB} (m)	H (m)	A (m^2)
Façade	0.6	0.4	0.2	0.4
Floor	0.6	0.4	0.2	0.4

Table 3
Thermal transmittancy and dimensionless coefficients for the equivalent thermal wall of the façade.

U (W/m^2 K)	φ_{ii}	φ_{ie}	φ_{ee}
0.678	0.147	0.102	0.649

Table 4
Thermal coefficients of the different layers in the equivalent thermal wall of the façade.

Layer m	R_m (m^2 K/W)	C_m (kJ/m^2 K)	e_m (m)	k_m (W/m K)	ρ_m (kg/m^3)	$C_{p,m}$ (kJ/kg K)
S_i	0.13	–	–	–	–	–
1	0.236	217.169	0.1	0.424	2171.69	1
2	0.833	0.343	0.1	0.120	3.43	1
3	0.236	52.788	0.1	0.424	527.88	1
S_e	0.04	–	–	–	–	–
$\sum m_i$	1.475	270.3	0.3	–	–	–

Table 5
Thermal transmittancy and dimensionless coefficients for the equivalent thermal wall of the lower-floor slab.

U (W/m^2 K)	φ_{ii}	φ_{ie}	φ_{ee}
0.719	0.108	0.089	0.713

Table 6
Thermal coefficients of the different layers in the equivalent thermal wall of the lower-floor slab.

Layer m	R_m (m^2 K/W)	C_m (kJ/m^2 K)	e_m (m)	k_m (W/m K)	ρ_m (kg/m^3)	$C_{p,m}$ (kJ/kg K)
S_i	0.17	–	–	–	–	–
1	0.058	451.097	0.1	1.724	4510.96	1
2	1.004	0.303	0.1	0.099	3.03	1
3	0.058	71.70	0.1	1.724	717.01	1
S_e	0.10	–	–	–	–	–
$\sum m_i$	1.39	523.10	0.3	–	–	–

independent of the initial condition, the simulation is extended over a period of 4 days, being the solution of the last day used for the data analysis.

The time-dependent heat fluxes across the actual thermal bridge are obtained from the solution of Eq. (11) using the finite-volume method. Conversely, the efficient Laplace transform method [10] is used for the solution of the multilayered walls A and B and the equivalent thermal walls C and D as defined in Fig. 5. The comparison of both solutions is presented in Fig. 6: the independent analysis of the façade and the floor slab show a phase delay of about 2 h between both computation approaches. However, the analysis of both solutions for the thermal bridge ensemble presents a good agreement.

3.2. Joint between an intermediate-floor slab and a vertical wall

Fig. 7 depicts the geometry and thermal properties of the thermal bridge originated by the joint of a vertical wall with an intermediate-floor slab. The indoor spaces separated by the slab are habitable, and the outside surface of the vertical wall is in contact

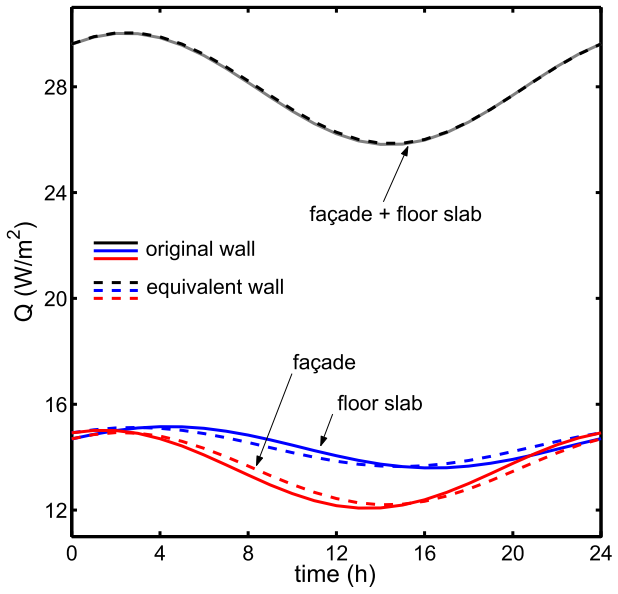

Fig. 6. Heat flux across the inner surface for the thermal bridge of the test case 3.1.

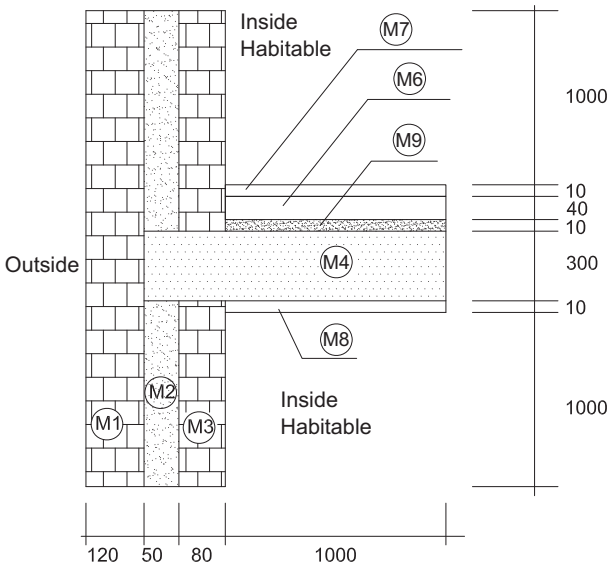

Fig. 7. Analysis of the layers of a thermal bridge created by the junction of an external façade and an intermediate floor slab, with both inner spaces habitable. Dimensions in mm.

with the ambient. A method to obtain the equivalent thermal wall of this thermal bridge topology is devised.

3.2.1. Adjustment of the method

In this thermal bridge, the intermediate-floor slab acts as a high-mass fin with high thermal inertia. This slab separates two indoor spaces with the same boundary conditions. In this case, the calculation method is based on the analysis of the energy stored in the thermal bridge and the heat flow towards the lower and higher indoor spaces. The steady-state heat conduction analysis provides the temperature field and the heat fluxes across the lower and higher slab surfaces. The total heat that penetrates across each surface is computed respectively as:

$$Q_h = \int_{S_h} q_{h,y}\,dx \tag{12}$$

$$Q_\ell = \int_{S_\ell} q_{\ell,y}\,dx \tag{13}$$

where S_h and S_ℓ are the higher and lower surfaces of the slab, $q_{h,y}$ is the wall heat flux across the higher surface of the slab and $q_{\ell,y}$ is the wall heat flux across the lower surface of the slab.

The fraction of the heat crossing each surface with respect to the total amount of energy that enters the slab is interpreted as the influence of the thermal bridge over the higher and lower inner spaces. Eqs. (14) and (15) are employed to assess this influence:

$$X_h = \frac{Q_h}{Q_h + Q_\ell} \tag{14}$$

$$X_\ell = \frac{Q_\ell}{Q_h + Q_\ell} \tag{15}$$

whereas the total energy stored in the thermal bridge is obtained as $E_{\text{tot}} = \int_S \rho C_p T dV$.

The location of the adiabatic plane over the slab, y_1, is computed using the definition of X_h and X_ℓ:

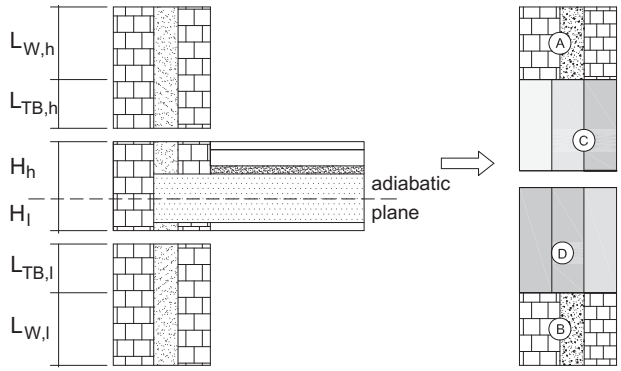

Fig. 8. Method for the adjustment of thermal inertias of the equivalent thermal wall for the junction of a façade and an intermediate floor slab.

$$E_\ell = X_\ell \int_{y_0}^{y_1} \rho C_p T \mathrm{d}V \tag{16}$$

$$E_h = X_h \int_{y_1}^{y_2} \rho C_p T \mathrm{d}V \tag{17}$$

The coordinate y_1 that defines this plane is depicted in Fig. 8. Eqs. (16) and (17) allow to obtain the values $H_h = y_2 - y_1$ and $H_\ell = y_1 - y_0$, which assess the influence of the thermal bridge over the higher and lower indoor spaces. Numerical quantities are reported in Table 7.

Unlike the previous case, the computation lengths defined in this thermal bridge are referenced to the outside levels. Therefore, the area of the thermal bridge is computed, both for the high and lower spaces. Tables 8 and 9 summarize the properties of the equivalent thermal wall C (higher façade). The quantities obtained for the equivalent thermal wall D (lower façade) are reported in Tables 10 and 11.

3.2.2. Results

The solution of the heat conduction equation Eq. (11) over the actual geometry of the thermal bridge has been obtained numerically and employed to compute the energy demand per unit of area in the higher and lower spaces, as well as the influence of the thermal bridge over the whole indoor space. Likewise, the analytical solution for the multi-layered equivalent thermal wall has been employed to accomplish the same post-processing routine. Comparison of both approaches are presented in Fig. 9, showing that both models present a very similar thermal dynamic response.

Table 7
Characteristic lengths of the thermal bridge created by intermediate-floor slab and façade.

	L_W (m)	L_{TB} (m)	H (m)	A (m^2)
Higher space	0.6	0.4	0.185	0.585
Lower space	0.6	0.4	0.185	0.585

Table 8
Thermal transmittancy and dimensionless coefficients for the equivalent thermal wall of the higher façade.

U (W/m^2 K)	φ_{ii}	φ_{ie}	φ_{ee}
0.647	0.468	0.136	0.111

Table 9
Thermal coefficients of the different layers in the equivalent thermal wall of the higher façade.

Layer m	R_m (m^2 K/W)	C_m (kJ/m^2 K)	e$_m$ (m)	k$_m$ (W/m K)	ρ_m (kg/m^3)	C$_{p,m}$ (kJ/kg K)
S_i	0.13	–	–	–	–	–
1	0.208	172.157	0.1	0.481	1721.57	1
2	0.959	0.019	0.1	0.104	0.19	1
3	0.208	95.624	0.1	0.481	956.24	1
S$_e$	0.04	–	–	–	–	–
$\sum m_i$	1.545	267.8	0.3	–	–	–

Table 10
Thermal transmittancy and dimensionless coefficients for the equivalent thermal wall of the lower façade.

U (W/m^2 K)	φ_{ii}	φ_{ie}	φ_{ee}
1.066	0.493	0.136	0.235

Table 11
Thermal coefficients of the different layers in the equivalent thermal wall of the lower façade.

Layer m	R_m (m^2 K/W)	C_m (kJ/m^2 K)	e_m (m)	k_m (W/m K)	ρ_m (kg/m^3)	C$_{p,m}$ (kJ/kg K)
S$_i$	0.13	–	–	–	–	–
1	0.097	334.46	0.1	1.031	3344.64	1
2	0.574	1.27	0.1	0.174	12.70	1
3	0.097	112.57	0.1	1.031	1125.66	1
S$_e$	0.04	–	–	–	–	–
$\sum m_i$	0.938	448.3	0.3	–	–	–

4. Definition of the thermal bridge

The analysis of thermal bridges and their handling in the calculation of thermal loads in HVAC studies are still unresolved issues in building energy simulation tools. Most of the standards currently existing (including ISO 10211-1:1995 [3] and ISO 10211-2:2001 [4]) consider the thermal bridges as constructive elements without thermal inertia, and therefore only the steady-state heat transfer analysis is a matter of study. The physical parameter that drives these modeling strategies is the linear thermal

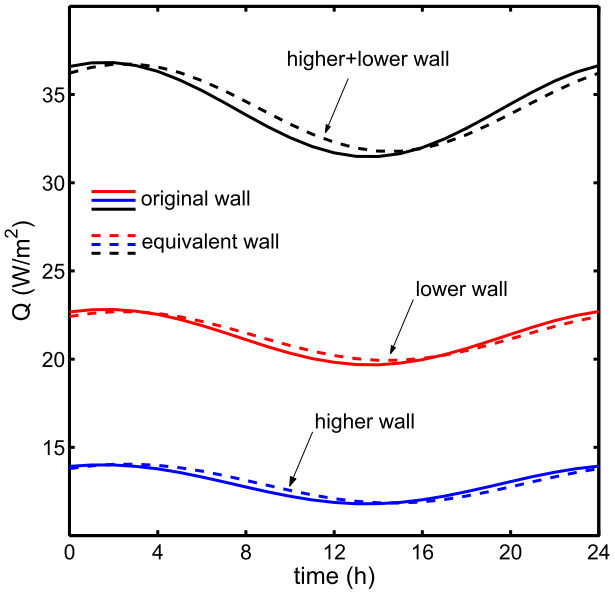

Fig. 9. Heat flux across the inner surface for the thermal bridge of the test case 3.2.

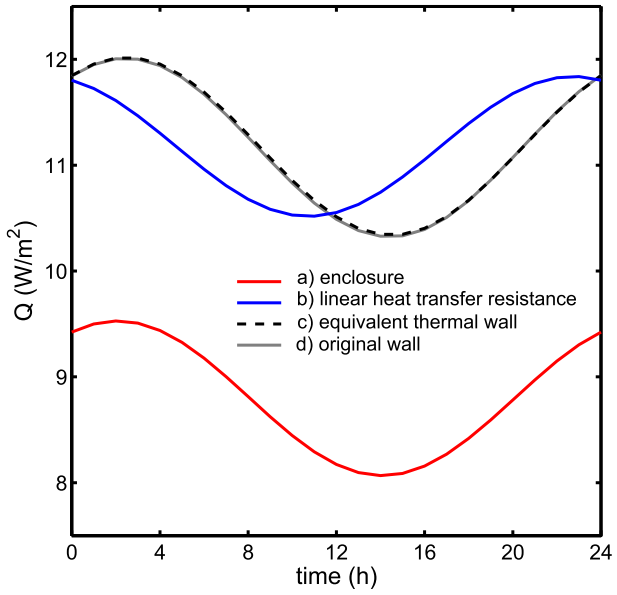

Fig. 10. Solution of the heat flux for different models of the thermal bridge.

transmittancy Ψ(W/m K). However, the high influence of the mass of some thermal bridges on their thermal inertia has an important impact on the dynamic response of the energy demand in buildings. In order to better understand the effect of the thermal inertia, four different dynamic responses of the wall heat flux in the thermal bridge of Section 3.1 (vertical wall and ground floor slab) are compared in Fig. 10, namely:

a) The model of the thermal bridge taking into account only the heat transfer across the enclosures, without considering the effect of the 2D temperature distribution.
b) The model of the thermal bridge as a linear heat transfer resistance without mass or thermal inertia, derived from a steady-state heat conduction analysis.
c) The solution of the analytical expressions for multilayered walls [10] applied to the three-layered equivalent thermal wall of the objective thermal bridge.
d) The finite-volume solution of the unsteady heat conduction problem in the objective thermal bridge, obtained with the software ANSYS.

The boundary conditions applied in the four cases are: indoor temperature $T_{int} = 20$ °C; fluctuating outside temperature $\widehat{T}_0 = F\sin(\omega t)$ over a 24 h period. The surface thermal resistances considered are: $R_{so} = 0.04$ m^2 K/W y $R_{si} = 0.13$ m^2 K/W for the vertical wall; and $R_{se} = 0.04$ m^2 K/W and $R_{si} = 0.1$ m^2 K/W for the slab. The analysis of the results clearly show that, if the thermal bridge is not properly considered -case a)-, the computation of the wall heat flux is underestimated in approximately 25% with regard to the actual performance of the thermal envelope. Conversely, if the thermal bridge is taken into account but only in steady-state and without thermal inertia -case b)-, the energy demand evolution retrieved by the model is substantially time-delayed with respect to real conditions. Only the simulation of the thermally-equivalent wall model (c) reproduces a dynamic response similar to that of the full analysis of the thermal bridge (d).

In order to implement this method (c) in building energy simulation programs, the software has to divide every wall in three parts. The part located in the center would be the thermally equivalent wall of the original wall (calculated by the classical equivalent wall method). The upper and lower parts of the wall would take into account the thermal bridge and therefore would be calculated by the equivalent wall method proposed in this article. A similar strategy would be applied for the modelling of floors and ceilings.

5. Conclusions

1. The equivalent thermal wall method is applicable to the modeling of high-inertial thermal bridges, provided that the thermal properties of the equivalent walls are properly determined.
2. An iterative algorithm has been devised to adjust the thermal properties of the equivalent thermal walls. This method is complemented with a thorough strategy to decompose the thermal bridge into several multi-layered walls.
3. The thermal bridge topologies formed by the junction of a vertical wall and an intermediate or a ground floor slab are analyzed with this approach. Two new equivalent thermal walls are created in each case, whose 1D-transient analysis is complemented with the study of the walls unaffected by the 2D heat flow induced by the thermal bridge junction.
4. The modeling of the thermal bridges following the method proposed in this work retrieves a reliable transient response of the problem. The good agreement of the results with the full simulation of the heat conduction problem across the thermal bridge actual geometry serves as a validation of the method.

Acknowledgements

We gratefully acknowledge the financial support of the CDTI (Centro para el Desarrollo Tecnológico Industrial) and the company CYPE Ingenieros.

References

[1] E.U., 2002/91/EC of the European Parliament and of the Council of 16th December 2002 on the Energy Performance of Buildings, 2002.
[2] S.A. Al-Sanea, M.F. Zedan, Effect of insulation location on initial transient thermal response of building walls, J. Build. Phys. 24 (2001) 275–300.
[3] EN ISO 10211-1:1995, Thermal Bridges in Building Construction. Heat Flows and Surface Temperatures. Part 1: General Calculation methods, 1995.
[4] EN ISO 10211-2:2001, Thermal Bridges in Building Construction – Calculation of Heat Flows and Surface Temperatures – Part 2: Linear Thermal Bridges, 2001.
[5] H. Erhorn, H. Erhorn-Kluttig, M. Citterio, M. Cocco, D. van Orshoven, A. Tilmans, P. Schild, P. Bloem, K. Engelund Thomsen, J. Rose, An Effective Handling of Thermal Bridges in the EPBD Context, Final Report of the IEE ASIEPI Work Thermal Bridges, ASIEPI Report, WP4, 2010.
[6] Y. Gao, J.J. Roux, L.H. Zhao, Y. Jiang, Dynamical building simulation: a low order model for thermal bridges losses, Energy Build. 40 (2008) 2236–2243.
[7] B.K. Karambakkam, B. Nigusse, J.D. Spitler, A one-dimensional approximation for transient multi-dimensional conduction heat transfer in building envelopes, in: The 7th Symposium on Building Physics in the Nordic Countries, Reykjavik, 2005.
[8] E. Kossecka, J. Kosny, Equivalent wall as a dynamic model of a complex thermal structure, J. Therm. Insul. Build. Envelopes 20 (1997) 249–268.
[9] E. Kossecka, Relationships between structure factors, response factors and z-transfer function coefficients for multi-layer walls, ASHRAE Trans. 104 (1A) (1998) 68–77.
[10] I.R. Maestre, P.R. Cubillas, L.P. Lombard, Transient heat conduction in multi-layer walls: an efficient strategy for Laplace's method, Energy Build. 42 (2010) 541–546.
[11] EnergyPlus Engineering Reference, The Reference To EnergyPlus Calculations, University of Illinois, U.S. Department of Energy, 2013.
[12] D.B. Crawley, L.K. Lawrie, F.C. Winkelmann, W.F. Buhl, Y.J. Huang, C.O. Pedersen, R.K. Strand, R.J. Liesen, D.E. Fisher, M.J. Witte, J. Glazer, EnergyPlus: creating a new-generation building energy simulation program, Energy Build. 33 (4) (2001) 319–331.
[13] LBNL, DOE-2 Engineer Manual-Version 2.1A, LBNL, University of California Berkeley, 1982.
[14] S.A. Al-Sanea, Finite-volume thermal analysis of building roofs under two-dimensional periodic conditions, Build. Environ. 38 (2003) 1039–1049.
[15] H.K. Versteeg, W. Malalasekera, An Introduction To Computational Fluid Dynamics, The Finite Volume Method, second ed., Pearson Prentice Hall, 2007.
[16] MathWorks INC, Matlab Version 7.9.0.529 Users Guide, 2009.
[17] Ansys INC, Ansys 11.0 Users Guide, 2007.